

# Photophysical studies of substituted 1,2-diarylethenes: twisted intramolecular charge transfer fluorescence in dimethoxycyano-substituted 1,2-diarylethene

2 PERKIN

Anil K. Singh\* and Sriram Kanvah

Department of Chemistry, Indian Institute of Technology, Bombay, Powai, Mumbai 400 076, India. E-mail: Retinal@ether.chem.iitb.ernet.in; Fax: (091-22) 576 7152

Received (in Cambridge, UK) 15th August 2000, Accepted 16th November 2000

First published as an Advance Article on the web 6th February 2001

1,2-Diarylethenes, namely (*E*)-1-(4-cyanophenyl)-2-phenylethene (**1**), (*E*)-1-(4-methoxyphenyl)-2-phenylethene (**2**), (*E*)-1-(3,4-dimethoxyphenyl)-2-phenylethene (**3**), (*E*)-1-(4-cyanophenyl)-2-(4-methoxyphenyl)ethene (**4**) and (*E*)-1-(4-cyanophenyl)-2-(3,4-dimethoxyphenyl)ethene (**5**), have been synthesized and their absorption and fluorescence properties at room temperature in different organic solvents and also in 1,4-dioxane–water binary mixtures have been investigated. Additionally, the fluorescence of these compounds has been examined at 77 K in an ethanol–methanol (1 : 1 v/v) matrix. Photophysical parameters like absorption, excitation and fluorescence spectra, fluorescence quantum yields, excited state dipole moment changes, and correlation of solvatochromic fluorescence with solvent parameters like  $E_T(30)$ -values and the  $\pi^*$ -scale have been made. Compound **5**, with one cyano and two methoxy substituents, has been found to exhibit solvent polarity-dependent dual fluorescence. The shorter wavelength fluorescence is attributed to an initially excited delocalized planar state, while the longer wavelength fluorescence is attributed to a non-planar twisted intramolecular charge transfer excited state.

## Introduction

Photoinduced intramolecular charge transfer has been implicated in a number of chemical and biological processes.<sup>1</sup> In this context, the photochemical and photophysical behaviour of substituted stilbene derivatives has attracted considerable attention in recent years.<sup>2</sup> In spectroscopic terms, the excited  $\pi-\pi^*$  singlet state ( $S_1$ ) of parent (*E*)-stilbene ((*E*)-1,2-diphenylethene, DPE) is of  $B_u$  type while the ground state is of  $A_g$  type. The covalent  $A_g$  state is insensitive to solvent polarity while an ionic  $B_u^+$  state is relatively stabilized in polar solvents. It is also known that the fluorescence from the  $S_1$  state competes with the activated twisting of DPE into a perpendicular ( $P^*$ ) geometry, which subsequently leads to *cis* and *trans* isomers.<sup>2</sup> However, in the fluorescence of donor–acceptor stilbenes, the existence of a double minimum potential for the excited state has been suggested.<sup>3</sup> One is due to the initially excited state in which the fluorophore has a planar geometry and is electronically delocalized. The second one is due to an excited state in which the fluorophore has a perpendicularly twisted geometry with full charge separation, and this non-planar excited state is referred to as the twisted intramolecular charge transfer (TICT) state.<sup>3</sup> The initially excited state with planar fluorophore geometry is separated from the non-planar TICT excited state by an activation barrier. As expected, this activation barrier decreases for polar solvents. Further, as the double bond twisted perpendicular species (the  $P^*$  state) is non-emissive, its rapid formation acts as a fluorescence quenching process on the emission from the primary planar excited state with correspondingly low fluorescence quantum yield in solvents of high polarity.

In diphenylpolyenes [ $Ar(CH=CH)_nAr$ ], the presence of single bond linked donor–acceptor groups and a near planar ground state geometry may help in the formation of the TICT excited state. However, the double bonds can also lead to *E–Z* isomerization, which can compete with TICT state formation. Among the stilbenoid systems, such TICT behaviour is observed in 4-*N,N*-dimethylamino-4'-cyanostilbene, as described using

picosecond time-resolved spectroscopy.<sup>4</sup> In such molecules, formation of fluorescent bicimer species resulting from the association of a pair of electronically excited states with large dipole moments has also been suggested. 4-*N,N*-Dimethylamino-4'-nitrostilbene has also been shown to exhibit TICT behaviour in polar solvents involving a twist of the nitro group orthogonal to the rest of the molecule.<sup>3d</sup> Among the higher members of diphenylpolyenes, substituted diphenylhexatrienes exhibit such a dual fluorescence phenomenon.<sup>5</sup> The exceptionally large solvatochromism in the fluorescence of nitro-substituted diphenylbutadienes has also been attributed to the charge transfer phenomenon in single bond twisted excited states.<sup>6</sup>

We now report that stilbene compounds containing cyano and methoxy groups on the aromatic ring are also capable of exhibiting dual fluorescence due to the TICT state. Thus, in this paper we describe the dual fluorescence characteristics of (*E*)-1-(4-cyanophenyl)-2-(3,4-dimethoxyphenyl)ethene (**5**) in comparison to other substituted stilbene compounds, namely (*E*)-1-(4-cyanophenyl)-2-phenylethene (**1**), (*E*)-1-(4-methoxyphenyl)-2-phenylethene (**2**), (*E*)-1-(3,4-dimethoxyphenyl)-2-phenylethene (**3**), (*E*)-1-(4-cyanophenyl)-2-(4-methoxyphenyl)ethene (**4**) (Fig. 1).

## Experimental

### Materials, apparatus and general procedures

DPE and all other chemicals used in the synthesis and fluorescence studies were from Aldrich. AR/Puriss grade organic solvents were obtained from SRL Pvt. Ltd. Mumbai and Spectrochem, Mumbai (India). Petroleum ether (60–80 °C fraction) was procured from other local dealers. All the solvents were thoroughly dried and freshly distilled prior to their use.<sup>7</sup> Chromatography grade silica gels were obtained from E. Merck (India) Ltd., Mumbai. Melting points were determined on a Veego melting point apparatus and are uncorrected. IR spectra were measured on an Impact 400 Nicolet FTIR

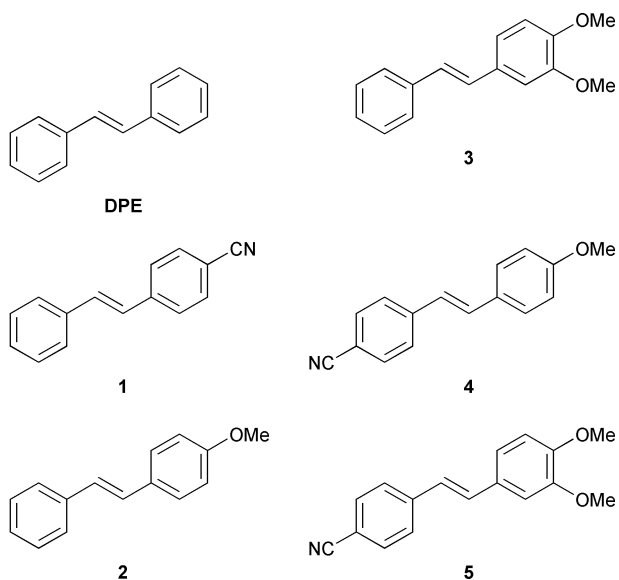


Fig. 1 Structures of compounds 1–5.

spectrophotometer. NMR spectra in  $\text{CDCl}_3$  were recorded on a Varian 300 MHz spectrometer using TMS as internal standard at the Regional Sophisticated Instrumentation Center, I.I.T. Bombay. Uv–vis spectra were measured on a Shimadzu UV-260 spectrophotometer. Steady state fluorescence measurements were carried out on a DM1B microprocessor controlled Spex-112 Fluorolog spectrofluorimeter having slit widths of 1 and 1.5 mm for excitation and emission monochromators respectively. The fluorescence spectra were recorded by exciting at the absorption maximum ( $\lambda_{\text{ab max}}$ ) and the excitation spectra were obtained by using the fluorescence maximum ( $\lambda_{\text{f max}}$ ) of the respective compounds. The fluorescence quantum yield ( $\phi_{\text{f}}$ ) was determined against quinine sulfate in 0.5 M  $\text{H}_2\text{SO}_4$  ( $\phi_{\text{f}}$ , 0.545) as standard.<sup>8</sup> The low temperature fluorescence studies in an ethanol–methanol matrix at 77 K were performed on a Spex-112 Fluorolog spectrofluorimeter equipped with Spex-1932 F accessories. For all electronic spectroscopic (absorption, fluorescence excitation and emission) studies,  $1.0 \times 10^{-5}$  M solutions of 1–5 were used. Solutions were purged with dry nitrogen prior to recording the fluorescence emission and excitation spectra. All the solutions were prepared and handled under protective dim-red light conditions to avoid unwanted exposure to light of the compounds under study.

## Synthesis

Compounds 1–5 were synthesized by following the modified Wittig–Horner reaction.<sup>9</sup> In a typical reaction procedure, a slight excess of triethyl phosphite was refluxed with the respective benzyl bromide in the presence of DMF to give the respective phosphonates. The freshly distilled phosphonates were slowly added to a stirring suspension of sodium methoxide and DMF in ice-cold conditions. The reaction mixture was stirred under nitrogen to allow the generation of the anion corresponding to the phosphonate. The aldehyde taken in dry DMF was slowly syringed into the reaction flask and the reaction mixture was further stirred at room temperature until maximum disappearance of the aldehyde as indicated by TLC (silica gel, 5% ethyl acetate in petroleum ether, 60–80 °C fraction). The reaction mixture was then poured into ice-cold brine. The precipitate so formed was filtered and further purified by column chromatography using 2% ethyl acetate in petroleum ether (60–80 °C fraction) as eluent.

Thus, 1 was obtained by the reaction of benzaldehyde with the phosphonate ester of cyanobenzyl bromide. Compounds 2 and 3 were obtained by the reaction of the phosphonate of benzyl bromide with 4-methoxybenzaldehyde and 3,4-dimethoxybenzaldehyde respectively.

Stilbenes 4 and 5 were prepared by the reaction of the phosphonate of cyanobenzyl bromide with 4-methoxy- and 3,4-dimethoxybenzaldehyde respectively.

## Physico-chemical characterization data for 1–5

**(E)-1-(4-Cyanophenyl)-2-phenylethene (1).** Yield 40%; mp 120–121 °C (lit.,<sup>10</sup> 115 °C); Uv–vis (MeCN),  $\lambda_{\text{max}}/\text{nm}$  ( $\epsilon$ ,  $1 \text{ mol}^{-1} \text{ cm}^{-1}$ ): 315 (17419); IR,  $\nu_{\text{max}}$  ( $\text{cm}^{-1}$ ): 3032, 2927, 2216, 1604, 1485, 966;  $^1\text{H NMR}$   $\delta$ : 7.09 (1H, d,  $J = 16.29$  Hz,  $\text{C}_6\text{H}_5\text{-CH=CH-}$ ), 7.22 (1H, d,  $J = 16.47$  Hz,  $\text{NC-C}_6\text{H}_4\text{-CH=CH-}$ ), 7.31–7.54 (m, 5H, phenyl protons), 7.57–7.64 (4H, AB quartet,  $J = 8.60$  Hz/2.07 Hz, cyanophenyl protons).

**(E)-1-(4-Methoxyphenyl)-2-phenylethene (2).** Yield 40%; mp 130–132 °C (lit.,<sup>10</sup> 136 °C); Uv–vis (MeCN),  $\lambda_{\text{max}}/\text{nm}$  ( $\epsilon$ ,  $1 \text{ mol}^{-1} \text{ cm}^{-1}$ ): 317 (27142); IR,  $\nu_{\text{max}}$  ( $\text{cm}^{-1}$ ): 3039, 2947, 1611, 1512, 1446, 972;  $^1\text{H NMR}$   $\delta$ : 3.83 (3H, s, methoxy protons), 6.90 (d of AB quartet,  $J = 8.79$  Hz/2.01 Hz, methoxyphenyl protons), 6.97 (1H, d,  $J = 16.29$  Hz,  $\text{C}_6\text{H}_5\text{-CH=CH-}$ ), 7.07 (1H, d,  $J = 16.29$  Hz,  $\text{MeO-C}_6\text{H}_4\text{-CH=CH-}$ ), 7.31–7.60 (m,  $-\text{C}_6\text{H}_5$ ), 7.46 (d of AB quartet,  $J = 8.79$  Hz/2.01 Hz, methoxyphenyl protons).

**(E)-1-(3,4-Dimethoxyphenyl)-2-phenylethene (3).** Yield 40%; mp 109–110 °C; Uv–vis (MeCN),  $\lambda_{\text{max}}/\text{nm}$  ( $\epsilon$ ,  $1 \text{ mol}^{-1} \text{ cm}^{-1}$ ): 325 (35416); IR,  $\nu_{\text{max}}$  ( $\text{cm}^{-1}$ ): 2950, 2889, 1577, 1530, 958;  $^1\text{H NMR}$   $\delta$ : 3.95 (3H, s, 3-methoxy protons), 3.90 (3H, s, 4-methoxy protons), 6.97 (1H, d,  $J = 16.29$  Hz,  $\text{C}_6\text{H}_5\text{-CH=CH-}$ ), 7.07 (1H, d,  $J = 14.10$  Hz,  $(\text{MeO})_2\text{-C}_6\text{H}_3\text{-CH=CH-}$ ), 6.87–7.5 (5H, m, aromatic protons).

**(E)-1-(4-Cyanophenyl)-2-(4-methoxyphenyl)ethene (4).** Yield 70%; mp 146–147 °C (lit.,<sup>11</sup> 149 °C); Uv–vis (MeCN),  $\lambda_{\text{max}}/\text{nm}$  ( $\epsilon$ ,  $1 \text{ mol}^{-1} \text{ cm}^{-1}$ ): 334 (40 277); IR,  $\nu_{\text{max}}$  ( $\text{cm}^{-1}$ ): 3010, 2935, 2842, 2225, 980; NMR  $\delta$ : 3.84 (3H, s, methoxy protons), 6.95 (1H, d,  $J = 16.12$  Hz,  $(\text{MeO})_2\text{-C}_6\text{H}_3\text{-CH=CH-}$ ), 7.17 (1H, d,  $J = 16.48$  Hz,  $\text{NC-C}_6\text{H}_4\text{-CH=CH-}$ ), 7.47–6.92 (4H, AB quartet,  $J = 8.79$  Hz/1.83 Hz, methoxyphenyl protons), 7.62–7.55 (4H, AB quartet,  $J = 8.43$  Hz/2.10 Hz, cyanophenyl protons).

**(E)-1-(4-Cyanophenyl)-2-(3,4-dimethoxyphenyl)ethene (5).** Yield 50%; mp 102–103 °C; Uv–vis (MeCN),  $\lambda_{\text{max}}/\text{nm}$  ( $\epsilon$ ,  $1 \text{ mol}^{-1} \text{ cm}^{-1}$ ): 348 (42 000); IR,  $\nu_{\text{max}}$  ( $\text{cm}^{-1}$ ): 3026, 2966, 2848, 2229, 1025;  $^1\text{H NMR}$   $\delta$ : 3.92 (3H, s, 4-methoxy protons), 3.96 (3H, s, 3-methoxy protons), 6.89–7.10 (3H, m, methoxyphenyl protons), 6.95 (1H, d,  $J = 16.10$  Hz,  $(\text{MeO})_2\text{-C}_6\text{H}_3\text{-CH=CH-}$ ), 7.16 (1H, d,  $J = 16.50$  Hz,  $\text{NC-C}_6\text{H}_4\text{-CH=CH-}$ ), 7.62–7.56 (4H, AB quartet,  $J = 8.42$  Hz/1.83 Hz, cyanophenyl protons).

## Results and discussion

### Absorption and fluorescence spectra in organic solvents

The uv–vis absorption and fluorescence spectral data of 1–5 in organic solvents are presented in Tables 1 and 2. As compared to the parent (*E*)-stilbene (DPE), which absorbs maximally at 293 nm in most of the organic solvents, the absorption maximum ( $\lambda_{\text{ab max}}$ ) of compounds 1–5 is red-shifted. However, the absorption changes of these compounds are largely insensitive to solvent polarity. The substituent-based red shift in  $\lambda_{\text{ab max}}$  of 1–5 as compared to DPE can be due to mesomeric effects. The presence of a substituent on the phenyl ring can cause an increase in the resonance delocalization of  $\pi$  electrons. Accordingly, a progressive shift in the  $\lambda_{\text{ab max}}$  is observed. Among compounds 1–5, the largest  $\lambda_{\text{ab max}}$  of 348 nm is observed for 5, which is substituted by cyano and two methoxy groups.

Like absorption spectra, the fluorescence excitation spectra of 1–5 are also found to be largely insensitive to the solvent

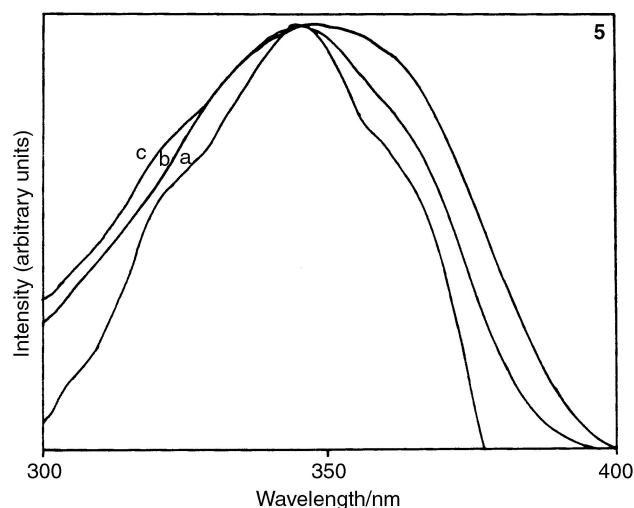
**Table 1** UV-vis absorption and fluorescence data of compounds **1** and **2**

Compound	Solvent	$\lambda_{ab\ max}/nm$	$\lambda_{f\ max}/nm$	$\lambda_{ex\ max}/nm$	$\phi_f$	Stokes' shift/cm <sup>-1</sup>
<b>1</b>	<i>n</i> -Heptane	315	365	323	0.010	4348
	1,4-Dioxane	317	376	327	0.015	4949
	THF	316	380	326	0.008	5329
	MeCN	315	387	317	0.005	5906
	MeOH	315	387	321	0.007	5906
	DMF	318	389	322	0.010	5739
<b>2</b>	<i>n</i> -Heptane	317	365	316	0.011	4148
	1,4-Dioxane	319	378	322	0.013	4892
	THF	319	376	316	0.007	4752
	MeCN	316	377	317	0.004	5120
	MeOH	315	384	315	0.005	5704
	DMF	316	379	313	0.010	5260

DPE:  $\lambda_{f\ max}/nm$ , 350–352;  $\phi_f$  is 0.022, 0.016, 0.014, 0.011 in *n*-heptane, 1,4-dioxane, MeOH and MeCN respectively.  $\lambda_{ab\ max}$ , absorption maximum;  $\lambda_{f\ max}$ , fluorescence maximum;  $\lambda_{ex\ max}$ , excitation maximum.

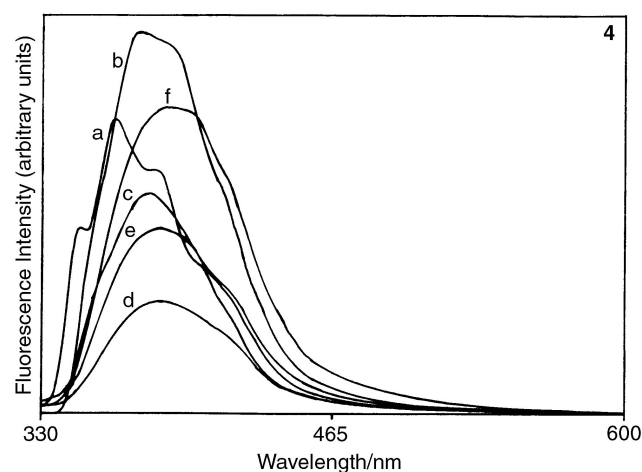
**Table 2** UV-vis absorption and fluorescence data of compounds **3–5**

Compound	Solvent	$\lambda_{ab\ max}/nm$	$\lambda_{f\ max}/nm$	$\lambda_{ex\ max}/nm$	$\phi_f$	Stokes' shift/cm <sup>-1</sup>
<b>3</b>	<i>n</i> -Heptane	323	374	322	0.033	4221
	1,4-Dioxane	325	385	322	0.031	4795
	THF	326	387	321	0.019	4835
	MeCN	323	399	318	0.013	5897
	MeOH	321	387	316	0.017	5312
	DMF	327	397	321	0.022	5392
<b>4</b>	<i>n</i> -Heptane	337	387	333	0.003	3833
	1,4-Dioxane	336	418	335	0.003	5838
	THF	338	419	334	0.003	5719
	MeCN	334	420	333	0.003	6130
	MeOH	335	420	333	0.004	6041
	DMF	339	422	332	0.005	5801
<b>5</b>	<i>n</i> -Heptane	348	416/410	342	0.007	4345
	1,4-Dioxane	348	422	340	0.012	5038
	THF	348	422	345	0.013	5038
	MeCN	346	443/468	343	0.014	6328
	MeOH	350	443/473	341	0.018	5998
	DMF	350	440/469	343	0.014	5844

**Fig. 2** Excitation spectra of **5** in: a) *n*-heptane, b) acetonitrile and c) methanol.

polarity. The fluorescence excitation spectra of **5** in *n*-heptane, acetonitrile and methanol are presented in Fig. 2 as typical examples. These absorption and excitation spectral data (Tables 1 and 2) clearly point towards a largely non-polar character of the ground state of these compounds.

In contrast to a rather weak solvent polarity effect on  $\lambda_{ab\ max}$ , a considerable red shift in the fluorescence maximum ( $\lambda_{f\ max}$ ) of **1–5** with increasing solvent polarity is observed, as compared to

**Fig. 3** Fluorescence spectra of **4** in: a) *n*-heptane, b) 1,4-dioxane, c) THF, d) MeCN, e) MeOH, f) DMF.

DPE, which fluoresces maximally at 350–352 nm. The red shift in  $\lambda_{f\ max}$  also depended on the substitution type. Fluorescence spectra of cyano-methoxy substituted **4** and **5** in various organic solvents are presented in Figs. 3 and 4. Upon changing the polarity of the solvent, the  $\lambda_{f\ max}$  of stilbenes substituted either with donor or acceptor groups (e.g. **1–3**) showed shifts ranging from 14–25 nm. The presence of both donor and acceptor substituents (as in compound **5** having cyano as an acceptor and two methoxy groups as donor groups) led to an increased solvatochromism. Compound **5** exhibits a larger shift

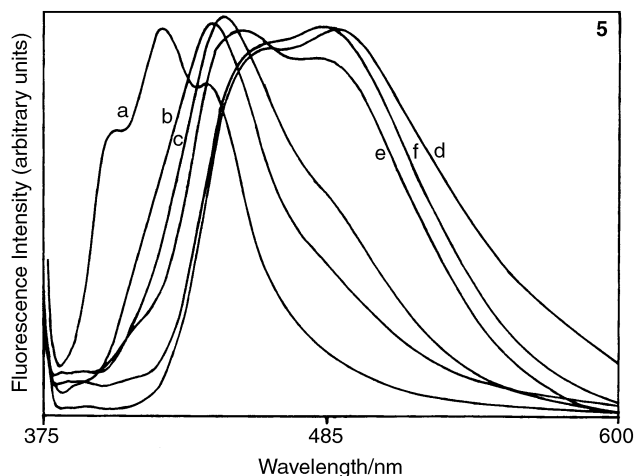


**Fig. 4** Fluorescence spectra of **5** in: a) *n*-heptane, b) 1,4-dioxane, c) THF, d) MeCN, e) MeOH, f) DMF.

(59 nm) as compared to compound **4** (35 nm) having cyano as an acceptor and only one methoxy as a donor. The solvent-dependent red shift in  $\lambda_{f \max}$  can be attributed to stabilization of the fluorescent excited state in a polar solvent (having a relatively higher relative permittivity).

Compound **5** has only one prominent fluorescence band in non-polar solvents. However, in polar solvents it exhibits an additional band at higher wavelength. This solvent polarity-based dual fluorescence of **5** is interesting and the shorter wavelength emission can be attributed to the initially excited planar, delocalized state while the longer wavelength emission can be due to the non-planar TICT state. Such dual emission characteristics are not observed in DPE and **1–4**. A single bond twist in the excited state of **5** can originate due to its electronically asymmetrical nature. The presence of donor–acceptor groups of unequal potential, *i.e.* dimethoxy as a very strong donor and cyano as a rather weak acceptor, can destabilize the system leading to twist across a single bond with consequent charge transfer in the excited state.

The bond twisting in excited **5** can occur at three possible sites. These are: a) the single bonds connecting the methoxy groups to the phenyl ring; b) the double bond; and c) the single bond connecting the phenyl ring and the double bond. The cyano group, being linear, is not considered for a possible twist. Using one of the twist pathways, the molecule tends to get stabilized. Though the exact position of bond twist is not known at present, it can be suggested that it occurs predominantly around one of the single bonds adjacent to the double bond as depicted in Fig. 5. It may be noted that the possibility of a double bond twist cannot be completely ruled out, as it is known to take place in stilbene compounds in time domains of  $\sim 100$  fs.<sup>2</sup> Further time-resolved fluorescence and photoisomerization studies of these compounds together with photochemical and photophysical studies involving bridged systems may throw light on the exact twist involved in the observed TICT process of arylethenes.

To further characterize the TICT excited state of **5**, the dependence of Stokes' shift on the solvent polarity has been correlated in terms of solvent parameters like Dimroth's parameter,<sup>12</sup>  $E_T(30)$  and the Kamlet–Taft  $\pi^*$  scale.<sup>13</sup> Dimroth and Reichardt and co-workers have proposed a solvent polarity parameter,  $E_T(30)$ , based on the transition energy for the longest-wavelength solvatochromic absorption band of the pyridinium-*N*-phenoxide betaine dye.<sup>12</sup> The  $E_T(30)$ -value for a solvent is defined as the transition energy of the dissolved betaine dye measured in kcal mol<sup>-1</sup>. The  $E_T(30)$ -values of several solvents are available in ref. 12. In general, the  $E_T(30)$ -values exhibit a good, mostly linear correlation with a solvent-sensitive process. Kamlet and Taft and co-workers have

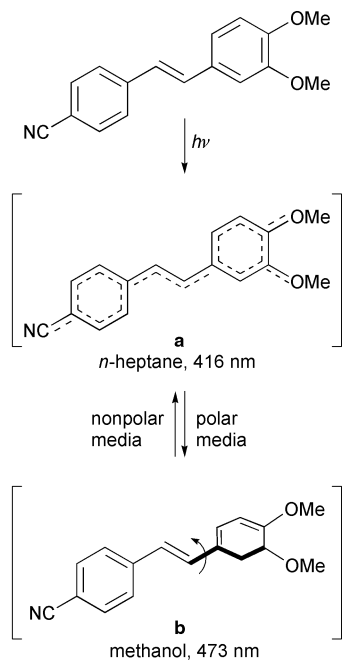


**Fig. 5** Plausible fluorescent excited state structures for **5**: a) Initially excited delocalized, planar state, and b) non-planar TICT state.

**Table 3** Dependence of spectral data of Fig. 6a and 6b on solvent polarity parameters

Compound	$E_T(30)$		$\pi^*$		$\Delta\mu/D$
	<i>R</i>	Slope	<i>R</i>	Slope	
<b>1</b>	0.8765	63.5	-0.9538	$2.43 \times 10^{-04}$	8.93
<b>2</b>	0.9419	57.55	-0.8368	$1.04 \times 10^{-04}$	7.47
<b>3</b>	0.7444	50.55	-0.9334	$2.85 \times 10^{-04}$	8.20
<b>4</b>	0.7100	68.49	-0.9538	$3.60 \times 10^{-04}$	8.99
<b>5</b>	0.8515	73.93	-0.8205	$3.39 \times 10^{-04}$	10.40

*R*: Linear correlation.  $\Delta\mu$ : Dipole moment change as obtained by Lippert–Mataga plot.

introduced the  $\pi^*$ -scale of solvent dipolarity/polarizability.<sup>13</sup> The  $\pi^*$ -scale is derived from solvent effects on the  $\pi \rightarrow \pi^*$  electronic transitions of a variety of nitroaromatics. Solvent effects on the  $\bar{\nu}_{\max}$ -values of several nitroaromatic-based solvatochromic indicators have been employed in the initial construction of the  $\pi^*$ -scale, which has been further expanded and refined by multiple least-squares correlations with additional solvatochromic indicators. In this way, an averaged  $\pi^*$ -scale of solvent dipolarity/polarizability has been established. This  $\pi^*$ -scale measures the ability of the solvent to stabilize a charge or a dipole by virtue of its dielectric effect.<sup>13</sup>

A plot of Stokes' shift vs.  $E_T(30)$ -values (Fig. 6a) shows that the Stokes' shift linearly increases with solvent polarity though the extent of the shift varies, as expected for a polar excited state in surroundings of differing electronic effects and relative permittivity. Similarly when emission maximum wavenumber ( $\bar{\nu}_{f \max}$ ) is plotted against  $\pi^*$ -scale, linear correlations for all the substituted stilbene compounds **1–5** are obtained (Fig. 6b). Compounds **4** and **5** containing donor–acceptor substituents show relatively larger Stokes' shifts (particularly in polar solvents) and hence the corresponding relatively larger slope (Table 3). These studies point towards a dipolar nature of the excited state responsible for the observed fluorescence.

Further experimental evidence in support of a dipolar character of the excited state concerned was obtained by calculation of excited state dipole moment changes ( $\Delta\mu$ ). As mentioned earlier, upon increasing the solvent polarity, the fluorescence spectrum shifts towards longer wavelengths, though the amount of the shift depends on the substitution type. This solvent

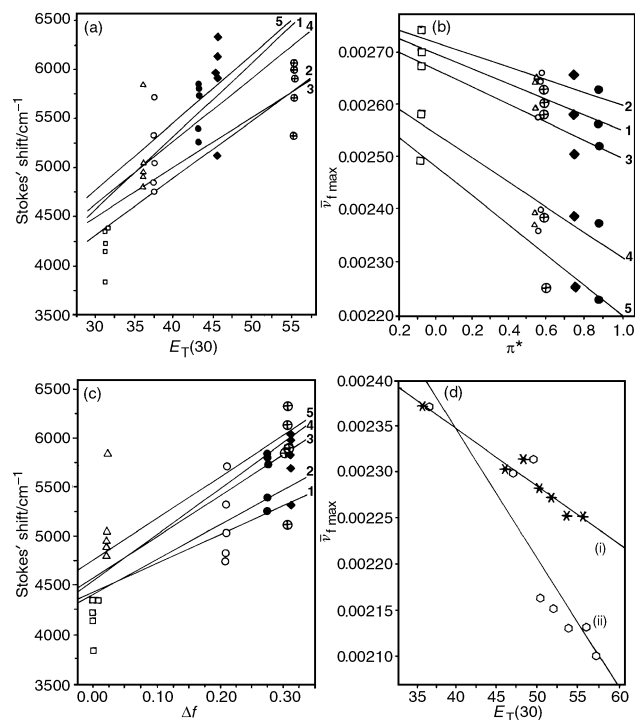


**Fig. 6** (a) Plots of Stokes' shift of 1–5 vs. Dimroth's solvent parameter  $E_T(30)$  in various solvents. (b) Plots of  $\bar{\nu}_{f \max}$  vs. Kamlet–Taft  $\pi^*$ -scale for 1–5. (c) Lippert–Mataga plot of Stokes' shift of 1–5 vs. solvent parameter ( $\Delta f$ ). [Solvents are: *n*-heptane ( $\square$ ); 1,4-dioxane ( $\Delta$ ); THF ( $\circ$ ); DMF ( $\bullet$ ); MeCN ( $\blacklozenge$ ); MeOH ( $\oplus$ )]. (d) Plots of  $\bar{\nu}_{f \max}$  of **5** (in 1,4-dioxane containing varying amounts of water) vs. Dimroth's solvent parameter  $E_T(30)$ : (i) due to delocalized, planar initially excited state; (ii) due to non-planar TICT excited state. Data points correspond to increasing amounts (from 0 to 70%) of water in 1,4-dioxane.

polarity-induced shift has been used to determine the change in dipole moment using the Lippert–Mataga equation:<sup>14</sup>  $\nu_a - \nu_f = \{[2(\mu_e - \mu_g)^2/hca^3] F(D, n)\}$ , where  $\nu_a - \nu_f$  is Stokes' shift,  $\mu_e$  and  $\mu_g$  are excited state and ground state dipole moments respectively,  $\mu_e - \mu_g = \Delta\mu$  (change in dipole moment),  $h$  is the Planck constant,  $c$  is the velocity of light,  $a$  is the Onsager radius, and  $F(D, n) = \Delta f$  is the solvent polarity parameter. Further,  $\Delta f = (D - 1)/(2D + 1) - (n^2 - 1)/(2n^2 + 1)$  where  $D$  is the relative permittivity and  $n$  is the refractive index of the solvent. For the Onsager radius parameter, we have used the molecular volume of 207.6 Å<sup>3</sup>, a reported value that has been obtained using molecular graphics and pseudoelectron density function calculations for similar stilbene compounds (e.g. 4-methoxy-4'-nitrostilbene).<sup>15</sup> Though the calculated molecular volumes are approximate, use of these values has been made in determining the excited state dipole moment changes in substituted stilbene compounds. It may, however, be mentioned that since the molecular volumes used are approximate, the dipole moment changes determined are approximate too. The plot of solvent polarity parameter  $\Delta f$  vs. Stokes' shift is shown in Fig. 6c and the changes in dipole moment ( $\Delta\mu$ ) thus obtained are given in Table 3. Among the stilbene compounds studied here, compound **5** shows the largest  $\Delta G$  value which is consistent with the presence of donor as well as acceptor groups.

A relatively large scattering of data points in some of the plots is observed, which could be due to other specific solvent–solute interactions occurring in surroundings of differing stereo-electronic features and relative permittivity.<sup>12b</sup>

#### Fluorescence studies in 1,4-dioxane–water binary mixtures

To demonstrate the gradual change of fluorescence emission with increase of solvent polarity, fluorescence studies of compounds 1–5 were done in 1,4-dioxane–water binary mixtures. The emission data obtained are tabulated in Tables 4 and 5. In the case of compound **5**, it is observed that as the concentration of water in 1,4-dioxane is increased to 30%, a second emission

band as a shoulder at around 463 nm starts appearing. A further increase in water concentration in 1,4-dioxane resulted in the appearance of a prominent emission band at around 465–475 nm. The shorter and longer wavelength emissions can respectively be attributed to the initially excited planar state and the TICT non-planar excited state of **5**. It is possible that solvent stabilization allows the TICT state to be populated from the initially excited planar delocalized species. Compounds 1–4 do not show such dual fluorescence characteristics in the 1,4-dioxane–water binary system.

A plot of fluorescence maximum wavenumber ( $\bar{\nu}_{f \max}$ ) for **5** in 1,4-dioxane–water binary solvent systems vs. the  $E_T(30)$ -values of the binary solvent system for both the fluorescence bands is shown in Fig. 6d. The data points correspond to the increasing amounts of water (zero to 70%) in 1,4-dioxane, which is linearly correlated with  $E_T(30)$ -values of the binary solvent mixtures. The  $E_T(30)$ -values were calculated according to the formula:  $Z/\text{kcal mol}^{-1} = 1.337 \times E_T(30)/\text{kcal mol}^{-1} + 9.80$  discussed in ref. 12(b), p. 388. The  $Z$ -values for various binary mixtures of 1,4-dioxane–water systems were taken as reported elsewhere.<sup>16</sup> The correlation parameters of the two plots are as follows: (a) for the fluorescence band due to the planar excited state (shorter wavelength band): linear correlation parameter,  $R = -0.9782$ , number of data points ( $N$ ) = 7 corresponding to seven solvent systems used, slope =  $7.5 \times 10^{-6}$ ; and (b) for the non-planar TICT band (longer wavelength band):  $R = -0.9071$ ,  $N = 7$ , slope =  $1.66 \times 10^{-5}$ . As expected, the slope for the band due to the non-planar TICT band is greater than that for the normal emission band due to the planar initially excited state. These data point towards relatively greater stabilization of the excited state responsible for the long wavelength emission and it can be attributed to a TICT state, which is expected to be stabilized in polar media.

#### Effect of solvent polarity on fluorescence quantum yields

As compared to DPE, the  $\phi_f$  of substituted stilbene compounds

**Table 4** UV-vis absorption and fluorescence data of compounds **1** and **2** in 1,4-dioxane–water binary mixtures

Compound	% Water in 1,4-dioxane	$\lambda_{ab\ max}/nm$	$\lambda_{f\ max}/nm$	$\lambda_{ex\ max}/nm$	Stokes' shift/cm <sup>-1</sup>
<b>1</b>	0	316	376	327	5049
	10	317	394	326	6165
	20	318	397	326	6257
	30	319	394	323	5967
	40	318	392	323	5936
	50	318	395	322	6130
<b>2</b>	60	319	392	320	5837
	0	319	377	322	4822
	10	319	395	321	6031
	20	319	378	321	4892
	30	318	390	317	5805
	40	319	387	316	5508
	50	318	386	317	5539
	60	317	393	317	6100

**Table 5** UV-vis absorption and fluorescence data of compounds **3–5** in 1,4-dioxane–water binary mixtures

Compound	% Water in 1,4-dioxane	$\lambda_{ab\ max}/nm$	$\lambda_{f\ max}/nm$	$\lambda_{ex\ max}/nm$	Stokes' shift/cm <sup>-1</sup>
<b>3</b>	0	326	386	324	4768
	10	326	401	324	5737
	20	326	396	323	5422
	30	325	396	321	5516
	40	325	394	321	5388
	50	325	399	320	5706
<b>4</b>	60	324	395	322	5547
	0	336	414	327	5607
	10	337	423	332	6032
	20	339	421	332	5745
	30	338	420	333	5776
	40	338	425	330	6056
<b>5</b>	50	337	427	330	6254
	0	348	422	348	5038
	10	348	430	348	5479
	20	348	432	345	5578
	30	348	438/463	343	5904
	40	347	440/465	347	6091
	50	348	444/470	345	6213
	60	346	444/469	343	6379
	70	347	475	341	7765

**Table 6** UV-vis absorption and fluorescence data of DPE and **1–5** in 1:1 ethanol–methanol matrix

Compound	$\lambda_{ab\ max}/nm$	Room temperature (~298 K)			Liquid N <sub>2</sub> (~77 K)		
		$\lambda_{f\ max}/nm$	$\lambda_{ex\ max}/nm$	$\phi_f$	$\lambda_{f\ max}/nm$	$\lambda_{ex\ max}/nm$	$\phi_f$
<b>DPE</b>	295	352	305	0.014	350	309	0.880
<b>1</b>	319	381	325	0.003	372	324	0.376
<b>2</b>	317	379	317	0.005	367	323	0.428
<b>3</b>	321	392	318	0.014	373	324	0.420
<b>4</b>	336	422	333	0.003	406	334	0.660
<b>5</b>	344	437/460	343	0.013	418	342	0.490

**1–5** are low, indicating rapid non-radiative transitions from the excited state. Solvent polarity does not significantly influence the  $\phi_f$  of these compounds (Tables 1 and 2). Among compounds **1–5**, **3** is the most and **4** is the least fluorescent in most of the solvents used. Further, a polar-protic solvent like methanol does not drastically reduce the fluorescence of these aryl-ethenes, as it does in the case of nitroaryldienes, which are reported to be very poorly fluorescent in methanol.<sup>6</sup> A slight increase in  $\phi_f$  of **5** in polar solvents (*e.g.*  $\phi_f = 0.007$  in *n*-heptane and 0.018 in methanol) can be due to the non-planar nature of the fluorescent species. Due to differences in dipole moment, an excited state is more stabilized in polar solvents than the ground state and therefore the transition from excited state to ground state will be slowed down in a polar solvent and enhanced in a less polar solvent, leading to the observed non-radiative losses.

#### Studies in ethanol–methanol glass at 77 K

Fluorescence studies of **1–5** at low temperature (77 K) were done in 1:1 (v/v) ethanol–methanol glass. As compared to room temperature, the  $\lambda_{f\ max}$  of **1–5** are considerably blue-shifted at 77 K (Table 6). Little or no change in fluorescence maximum with change in temperature is observed in DPE indicating the absence of any excited state geometry changes. The blue-shifted fluorescence at low temperature is found to vary with the substitution type. Compound **5** showed a shift of 32 nm from its long wavelength emission band. Further, the red-shifted emission band observed in polar solvents at room temperature disappeared at 77 K, indicating the existence of a non-planar TICT band at room temperature in polar solvents (Fig. 7). The  $\phi_f$  observed at 77 K is significantly greater than those observed at room temperature. The results suggest the

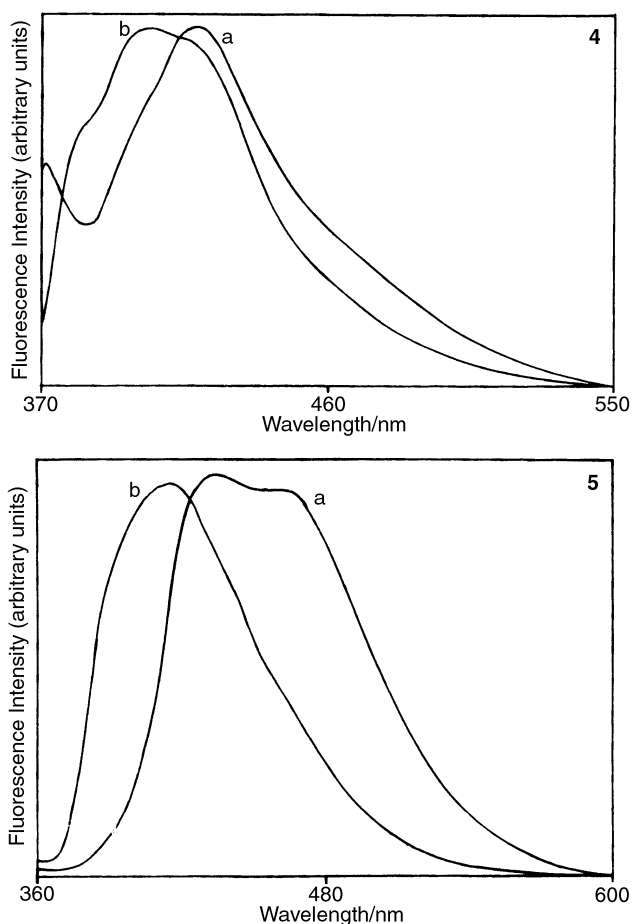


Fig. 7 Fluorescence of **4** and **5** at: (a) room temperature; (b) 77 K.

absence of any electronic motions and charge transfer in the rigid matrix. Apparently, the dual fluorescence observed at room temperature for **5** is non-existent at 77 K. This further enhances the evidence for TICT states in the fluorescence emission of **5**.

In conclusion, our results demonstrate that 1,2-diarylethenes having a linear acceptor group like  $-\text{CN}$  on one of the phenyl rings and two electron donor groups like  $-\text{OMe}$  on the other phenyl group are capable of solvent polarity-dependent dual fluorescence. The short wavelength fluorescence band is due to the initially excited state, which is electronically delocalized and has a planar geometry. The long wavelength fluorescence band is attributed to a non-planar TICT state having a dipolar character. However, it has not been possible to ascertain the exact site of excited state bond twist leading to the formation of TICT species. Besides providing further insight into the nature of the singlet excited state potential energy surface of diphenylpolyenes, the present results also give new directions for the development of newer fluorescence probes that can find applications as reporters of the microenvironment of organized chemical and biological systems.

## Acknowledgements

A research grant [37/7/95-R&D-II/559] from the Board of Research in Nuclear Sciences, Department of Atomic Energy, Government of India is gratefully acknowledged. We thank the reviewers of this paper for their valuable suggestions.

## References

- 1 W. Rettig, *Angew. Chem., Int. Ed. Engl.*, 1986, **25**, 971; W. Rettig and W. Majenz, *Chem. Phys. Lett.*, 1989, **154**, 335; A. W. Czarnik, *Frontiers in Supramolecular Organic Chemistry and Photochemistry*, VCH, Weinheim, Germany, 1991; W. Rettig and R. Lapouyade, *Fluorescence Probes Based on TICT States and Other Adiabatic Photoreactions*, in *Topics in Fluorescence Spectroscopy*, ed. J. R. Lakowicz, Vol. 4, *Probe Design and Chemical Sensing*, Plenum Press, New York, 1994; A. P. de Silva, H. Q. N. Gunaratne, T. Gunnlaugsson, A. J. M. Huxley, C. P. McCoy, J. T. Rademacher and T. E. Rice, *Chem. Rev.*, 1997, **97**, 1515.
- 2 M. T. Allen and D. G. Whitten, *Chem. Rev.*, 1989, **89**, 1691; J. Saltiel and Y.-P. Sun, *Cis-trans Isomerization of C=C Double Bonds*, in *Photochromism: Molecules and Systems*, ed. H. Durr and H. Bouas-Laurent, Elsevier, New York, 1990, p. 64; D. G. Waldek, *Chem. Rev.*, 1991, **91**, 415; H. Gerner and H. J. Kuhn, *Adv. Photochem.*, 1995, **19**, 1; T. Arai and K. Tokumaru, *Adv. Photochem.*, 1995, **20**, 1.
- 3 (a) W. Rettig, *Angew. Chem., Int. Ed. Engl.*, 1986, **25**, 971; (b) E. Gilibert, R. Lapouyade and C. Rulliere, *Chem. Phys. Lett.*, 1988, **145**, 262; (c) W. Rettig and W. Majenz, *Chem. Phys. Lett.*, 1989, **154**, 335; (d) H. Gruen and H. Gerner, *J. Phys. Chem.*, 1989, **93**, 7144; (e) M. van der Auweraer, Z. R. Grabowski and W. Rettig, *J. Phys. Chem.*, 1991, **95**, 2083.
- 4 E. Gilibert, R. Lapouyade and C. Rulliere, *Chem. Phys. Lett.*, 1991, **185**, 82.
- 5 C. T. Lin, H. W. Guan, R. K. McCoy and C. W. Spangler, *J. Phys. Chem.*, 1989, **93**, 39.
- 6 A. K. Singh, D. Manjula and S. Kanvah, *New J. Chem.*, 1999, **23**, 1075; A. K. Singh, D. Manjula and S. Kanvah, *J. Phys. Chem.*, 2000, **104**, 464.
- 7 W. L. F. Armarego and D. D. Perrin, *Purification of Laboratory Chemicals*, Butterworth-Heinemann, Oxford, 1996; B. S. Furniss, A. J. Hannaford, V. Rogers, P. W. G. Smith and A. R. Tatchell, *Vogel's Textbook of Practical Organic Chemistry Including Qualitative Organic Analysis*, ELBS and Longman, London, 1978.
- 8 W. H. Melhuish, *J. Phys. Chem.*, 1961, **65**, 229.
- 9 W. S. Wadsworth, Jr. and W. D. Emmons, *J. Am. Chem. Soc.*, 1961, **83**, 1733, 1961.
- 10 H. Jungman, H. Gusten and D. S. Frohlinde, *Chem. Ber.*, 1968, **101**, 2690.
- 11 V. Papper, D. Pines, G. Likhtenshtein and E. Pines, *J. Photochem. Photobiol. A: Chem.*, 1997, **111**, 87.
- 12 (a) K. Dimroth, C. Reichardt, T. Siepmann and F. Bohlmann, *Liebigs Ann. Chem.*, 1963, **661**, 1; (b) C. Reichardt, *Solvents and Solvent Effects in Organic Chemistry*, Verlag, Weinheim, Germany, 1990.
- 13 M. J. Kamlet, J.-L. M. Abboud and R. W. Taft, *J. Am. Chem. Soc.*, 1977, **99**, 6027; M. J. Kamlet, J.-L. M. Abboud, M. H. Abraham and R. W. Taft, *J. Org. Chem.*, 1983, **48**, 2877.
- 14 E. Lippert, *Z. Electrochem.*, 1957, **61**, 962; N. Mataga, Y. Kaifu and M. Koizumi, *Bull. Chem. Soc. Jpn.*, 1956, **29**, 465.
- 15 G. M. Anstead and J. A. Katzenellenbogen, *J. Phys. Chem.*, 1988, **92**, 6249.
- 16 E. M. Kosower, *J. Am. Chem. Soc.*, 1958, **80**, 3253; D. C. Turner and L. Brand, *Biochemistry*, 1968, **7**, 3381.